Schell, Juliana; Zyabkin, Dmitry; Lupascu, Doru C.; Hofsäss, Hans-Christian; Karabasov, Maksim O.; Welker, Andree; Schaaf, Peter:

A hyperfine look at titanium dioxide

Original published in:	AIP Advances / American Institute of Physics New York, NY : American Inst. of Physics. - 9 (2019), 8, art. 085208, 5 pp.
Original published:	2019-08-12
ISSN:	2158-3226
DOI:	10.1063/1.5097459
[*Visited:*	2019-11-13]

A hyperfine look at titanium dioxide

Cite as: AIP Advances 9, 085208 (2019); doi: 10.1063/1.5097459
Submitted: 26 March 2019 • Accepted: 5 July 2019 •
Published Online: 12 August 2019

J. Schell,[1,2,a)] D. Zyabkin,[3] Doru C. Lupascu,[2] Hans-Christian Hofsäss,[4] M. O. Karabasov,[2] A. Welker,[1] and P. Schaaf[3]

AFFILIATIONS

[1] European Organization for Nuclear Research (CERN), CH-1211 Geneva, Switzerland
[2] Institute for Materials Science and Center for Nanointegration Duisburg-Essen (CENIDE), University of Duisburg-Essen, 45141 Essen, Germany
[3] Chair Materials for Electrical Engineering and Electronics, Institute of Materials Science and Engineering, Institute of Micro and Nanotechnologies MacroNano®, TU Ilmenau, Gustav-Kirchhoff-Strasse 5, 98693 Ilmenau, Germany
[4] Georg-August-Universität Göttingen, Friedrich-Hund-Platz 1, 37077 Göttingen, Germany

[a)] Juliana Schell (juliana.schell@cern.ch)

ABSTRACT

Titanium dioxide is a commonly used material in a wide range of applications, due to its low price, and the increasing demand for it in the food- and pharmaceutical industries, and for low- and high-tech applications. Time-differential perturbed angular correlation (TDPAC) and Mössbauer spectroscopy measurements have a local character and can provide important and new information on the hyperfine interactions in titanium dioxide. With the application of characterization techniques and radioactive beams, these methods have become very powerful, especially for the determination of temperature dependence of hyperfine parameters, even at elevated temperatures. Such measurements lead to a better understanding of lattice defects and irregularities, including local environments with low fractions of particular defect configurations that affect electric quadrupole interactions. At ISOLDE-CERN, physicists benefit from the many beams available for the investigation of new doping configurations in titanium dioxide. We report the annealing study of titanium dioxide by means of the time differential perturbed γ-γ angular correlation of ^{111m}Cd/^{111}Cd in order to study the possible effects of vacancies in hyperfine parameters. This paper also provides an overview of TDPAC measurements and gives future perspectives.

I. INTRODUCTION

The time-differential perturbed correlation (TDPAC) technique[1] and Mössbauer spectroscopy[2] are very well suited for measuring the local charge distribution and the defect configurations of materials[3] over a wide temperature range. In parallel with the study of magnetic and electric hyperfine fields, the TDPAC method allows us to investigate the axial symmetry of electrostatic field gradients (EFGs). The perturbation of an angular correlation is due to an electric quadrupole interaction with nearby ions, bonding and conduction electrons, and the electronic shells of the TDPAC-probe ion. The Isotope mass Separator On-Line facility (ISOLDE)[4] can produce several types of probe ions. The 1.4-GeV proton beam at CERN bombards the ISOLDE target to produce isotopes, which are transferred to the ion source where they are ionized (Fig. 1). The beam is accelerated to 60 keV and separated by mass. The resulting pure beam is delivered to the beam line, where the implantation of TDPAC probes occurs. The concentration of the radioactive probes implanted at ISOLDE-CERN is so small that they have a negligible effect on the intrinsic properties of the titanium dioxide. The structural damage caused by the implantation process can be repaired after thermal treatment for a few minutes.

During a typical TDPAC experiment, two consecutive gamma rays, emitted by the same nucleus, are detected by photon counters. The emission of the first photon is isotropic, therefore, it is important to detect it in a selected direction. By detecting the emission of the second photon, a definite angular correlation with respect to the first gamma ray is observed. Furthermore, determining the time interval between the two emissions is essential, because during the lifetime of the intermediate state between gamma-ray emissions, the nucleus can interact with its surroundings and the angular correlation becomes perturbed. This leads to a time-dependent precession

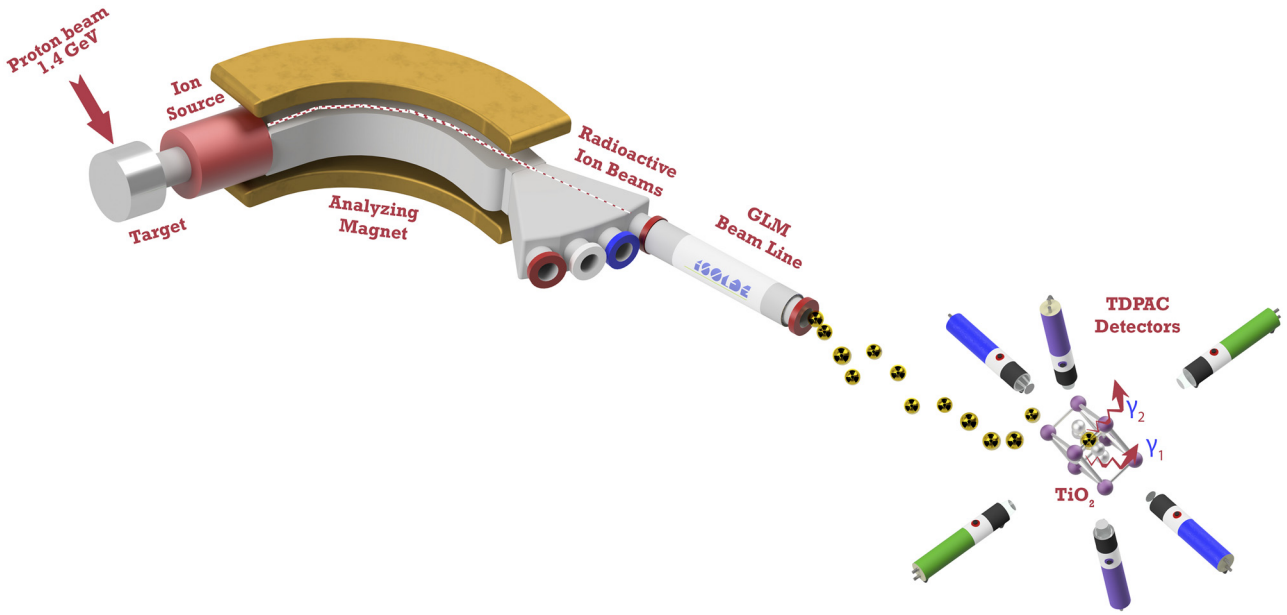

FIG. 1. Schematic of a typical online TDPAC spectroscopy setup at ISOLDE-CERN for ion implantation. The radioactive beam produced by ISOLDE is delivered to the beam line. The sample is placed inside the vacuum chamber, while the TDPAC detection system is placed outside it. For isotopes that are not too short lived, the measurements can be performed off-line.

of the angular correlation. Further information about analogue or digital TDPAC detection systems can be found in Refs. 5 and 6, and data evaluation formalism in Refs. 7 and 8.

Considering the nuclear spin I = 5/2 of the intermediate state, the perturbation factor for polycrystalline samples, for $\eta \neq 0$, is given by:

$$G_{22}(t) = s_0 + \sum_{n=1}^{3} s_n(\eta)\cos[\omega_n(\eta)t]. \quad (1)$$

ω_n are the transition frequencies between two M-states, $\omega_n = \left[E(M) - E(M')\right]/\hbar = 3\left|M^2 - M'^2\right|\omega_Q$. However, in the case of spin I = 1 for polycrystalline samples and $\eta \neq 0$, the degeneracy of the M-states is removed and the perturbation factor becomes:

$$G_{22}(t) = \frac{2}{5} + \frac{1}{5}\cos\omega_1 t + \frac{1}{5}\cos\omega_2 t + \frac{1}{5}\cos\omega_3 t, \quad (2)$$

with $\omega_1 = 2\eta\omega_Q$, $\omega_2 = (3-\eta)\omega_Q$, $\omega_3 = (3+\eta)\omega_Q$.

The transition frequencies are functions of the nuclear quadrupole frequency, which is defined by:

$$\omega_Q = \frac{eQV_{zz}}{4I(2I-1)\hbar}. \quad (3)$$

Here, Q is the nuclear quadrupole moment. Since the EFG is represented by a symmetrical and traceless (3x3) tensor, it can be fully characterized by the magnitude, V_{zz}, and the asymmetry parameter, $\eta = (V_{xx} - V_{yy})/V_{zz}$. η varies from 0 to 1, where 1 corresponds to maximal asymmetry. Coefficients s_n are only slightly dependent on η and are the amplitudes of the transition frequencies, ω_n. They are determined by the angle between the detectors if the EFG is randomly oriented, e g. in a polycrystalline sample. In single crystalline samples s_n also depends on the actual orientation of the EFG tensor with respect to the detectors. Additionally, δ is the relative half-width of the EFG distribution.[7]

Additional details of the formalism and the TDPAC technique can be found in Refs. 9–11. Different lattice effects, such as small thermal expansions and anisotropic thermal vibrations, contribute to variations in the asymmetry parameter. The data can be interpreted using *ab initio* codes,[12–14] including temperature dependence.[15]

A short literature review of previous TDPAC measurements for TiO_2 in the anatase and rutile phases, for investigations using ^{181}Hf and ^{111}In as probes, is described in Ref. 16. In addition to conventional isotopes, other works have successfully employed ^{44}Ti,[17,18] ^{111}Ag,[19] or, more recently, ^{111m}Cd.[20] Here we present an overview of TDPAC measurements, including ^{111}In experiments,[16,20–22] and new experimental results of single crystals after the implantation of ^{111m}Cd at ISOLDE-CERN. To our knowledge, measurements have never before been performed on annealing in an O_2 atmosphere and vacuum at 10^{-4} mbar.

II. AXIAL SYMMETRY OF THE ELECTRIC FIELD GRADIENT

Not only is the EFG different for the same probe, ^{111}Cd, if it originates from different parents (^{111}In, ^{111}Ag, or ^{111m}Cd), but the axial symmetry of the EFG also differs. Minor distortions of the angles from those of a pure TiO_2 lattice geometry can produce different η values. During the time window of the measurement, the nuclear quadrupole interaction takes place with either: (i) a Cd^{2+} ion that has a filled $4d^{10}$ electron configuration; (ii) a Ta^{5+} ion that has a filled $4f^{14}$ and an empty $5d^0$ electron configuration; or (iii) a

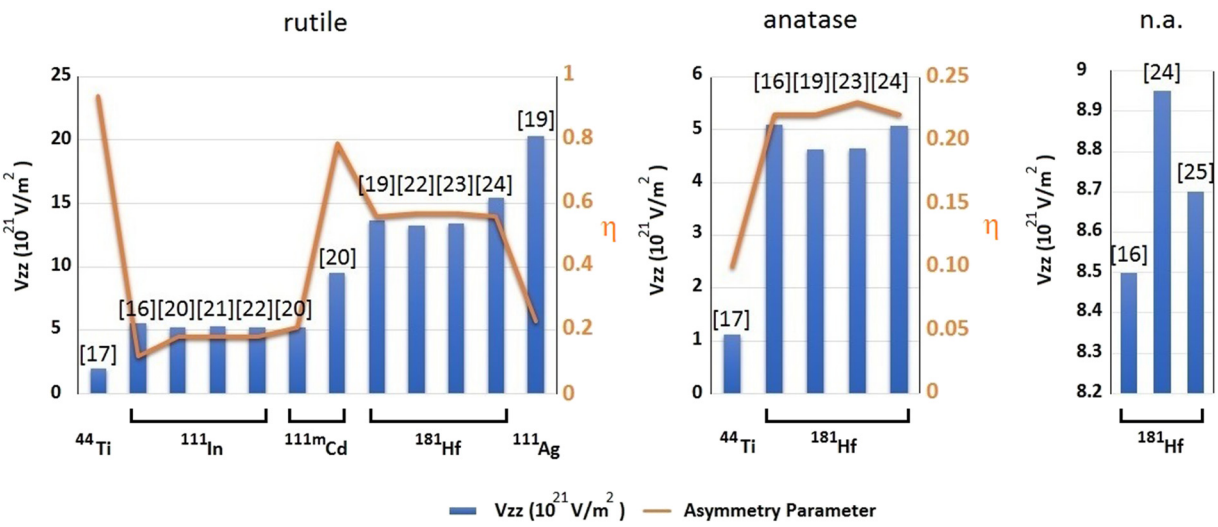

FIG. 2. Bar chart of reported values of Vzz and η for different TDPAC isotopes for rutile, anatase, and n.a. (additional local environment, which was not assigned to rutile or anatase).

Sc^{3+} ion with $3p^6$ and an empty $3d^0$ electron configuration. Using ^{111}In, previous studies obtained the value η ≈ 0.18 for rutile, whereas η = 0.23 was observed with ^{111}Ag. Studies profiting from the possibility of simultaneous ^{111}In and ^{111m}Cd implantation, which is currently possible only at ISOLDE, observed η = 0.175.[20] When only ^{111m}Cd was implanted, three sites were reported with η = 0.22, η = 0.79, and η = 0. Axial symmetry (η = 0) is expected in anatase due to its 4m2 crystal symmetry. However, η = 0.22(1) was reported for ^{181}Hf[19] after low-temperature annealing, which has been correlated with poor crystallinity. Figure 2 compares η and EFG values reported in previous work.

By considering ^{44}Ti in the rutile phase, Ryu *et al.* reported the strong dependence of η on the internal O position, *u*.[17] However, the large asymmetry parameter appears not to be affected by small variations in the internal lattice parameter. In addition, they observed discrepancies in the temperature dependence of the asymmetry parameters for Ti and Hf.

III. THE ELECTRIC FIELD GRADIENT

Only a single local environment was reported with the titanium/scandium probe[17,18] for rutile, although different fractions were observed after simultaneous ^{111}In + ^{111m}Cd implantations.[20]

Several reports used ^{181}Hf as probe nucleus.[16,19,22–24] Phase transitions from anatase to rutile have been studied with ^{181}Hf[24] and three different nuclear quadrupole interactions have been reported, one of which was not assigned to rutile or anatase, which assumes $V_{zz} \approx 9 \times 10^{21}$ V/m^2. Its origin was associated with the static inhomogeneity of the surface due to an uneven arrangement of oxygen bridging sites.[24] The same unknown local environment was observed in two other works, with $V_{zz} \approx 8.5 \times 10^{21}$ V/m^2 [16] and $V_{zz} \approx 8.7 \times 10^{21}$ V/m^2.[25] *Ab initio* calculations are, therefore, required to interpret the data. For the anatase phase, $V_{zz} \approx 4.6 \times 10^{21}$ V/m^2 was reported, while $V_{zz} \approx 14 \times 10^{21}$ V/m^2 was the average value assigned to the rutile structure. The values reported with ^{111}In can be found in Ref. 16. For instance, for room temperature the values for site 1 and 2 were $V_{zz} \approx 5.6 \times 10^{21}$ V/m^2 and $V_{zz} \approx 9.6 \times 10^{21}$ V/m^2, respectively.

A peculiar aspect of the nuclear quadrupole interactions observed for titanium dioxide is the increase of the quadrupole frequencies with temperature. This was clearly observed with the ^{181}Hf[16,22,29] and ^{44}Ti[18] probes. Since titanium is a very active getter,[26] this behavior offers strong evidence for oxygen diffusion from the surface. The diffusion effect has been previously studied for different temperature ranges in single crystals[27] and thin films.[28] However, the same effect has not been observed uniquely for ^{111}In.[22] Theoretical works show that Cd impurity induces anisotropic structural relaxations[14,15] on the nearest oxygen neighbors. The diffusion of oxygen into the host $Ti^{4+}O_2^{2-}$ is affected by distortions and lattice imperfections caused by the probes. With Sc incorporation, the cell volume tends to increase due to the ionic radius; however, this is an anisotropic process influenced by the number of O vacancies created by the heterovalent character of this probe.[30] It is expected that after Ta doping, the formation of Ti vacancies or Ti^{3+} is enhanced, whereas the formation of anionic vacancies, such as O vacancies, is suppressed. Therefore, competition between two diffusion processes must be considered. Thermal reduction is important from 875 °C[27] for the out-diffusion mechanism while the in-diffusion process takes place below that temperature and depends on the annealing atmosphere. Furthermore, re-oxidation and reduction effects are influenced by interstitial Ti, which becomes mobile from about 200 °C.[31] If the TDPAC probes are in the migration pathways, both diffusion processes will influence the perturbed angular correlation.

IV. PRE-DOPED SAMPLES

It is well known that doping can significantly alter the properties of titanium oxide, making it suitable for many applications.[32] To our knowledge, few works have reported on pre-doped titanium oxide samples measured by the TDPAC technique. For instance, doping with iron enhances its photocatalytic activity, allowing it

to absorb higher wavelengths of light.[33] Measurements carried out using ^{111}In in Fe-doped thin films[34] show only the paramagnetic state of the hyperfine interaction. These results agree with Mössbauer emission experiments[35] performed at ISOLDE-CERN, which also showed Fe^{3+} in the paramagnetic state.

Doping with an optimal concentration of Zr can lead to a higher photoactivity.[36] The reported mean values of the nuclear quadrupole interaction frequency and the asymmetry parameter measured using ^{181}Hf probes on Zr-doped rutile in Ref. 37 did not change significantly. However, the authors noted that the frequency distribution depends on the amount of Zr.

V. EXPERIMENTAL

TiO_2 (100) single crystals, of 99.6% purity, were obtained commercially from Goodfellow. The molten Sn target was installed at the General Purpose Separator (GPS) at ISOLDE-CERN for the production of a pure ^{111m}Cd beam. Room temperature ^{111m}Cd implantation at low dose, < 5x10^{11} atoms/cm^2, was performed at 30 kV. Following implantation, rapid thermal annealing (RTA) was performed at 873 K for 10 minutes in vacuum (10^{-4} mbar) or in a flux of O_2. Measurements were carried out at room temperature in air using an analogue TDPAC setup[1] equipped with four detectors with conical BaF_2 scintillators. The time resolution was 0.96 ns (FWHM). Theoretical perturbation functions were fitted to spectra using *Nightmare*[38] software to extract the hyperfine parameters.

VI. RESULTS AND DISCUSSION

The TDPAC spectra in Fig. 3 display a superposition of two quadrupole interaction signals. To aid discussion, the hyperfine parameters obtained will be quoted as A and B, corresponding to local environment 1 and 2, respectively, for measurements taken after annealing in vacuum.

The interaction (A) presents a well-defined electric quadrupole frequency δ = 8(3)% and an asymmetry parameter η = 0.22(1), corresponding to ω_0 = 101(3) Mrad/s. The fraction, f, of the crystalline site occupied by the TDPAC probe was 82(7)%. Similar frequency and asymmetry parameters have been reported previously[20] and attributed to Cd at the Ti-site. However, the reported fraction value was much lower (12%) than that reported in this work (82(7)%). This means that rapid thermal annealing at lower vacuum, (<10^{-4} mbar), could induce a much higher fraction for Cd at substitutional Ti-sites than the result reported for 10^{-5} mbar.

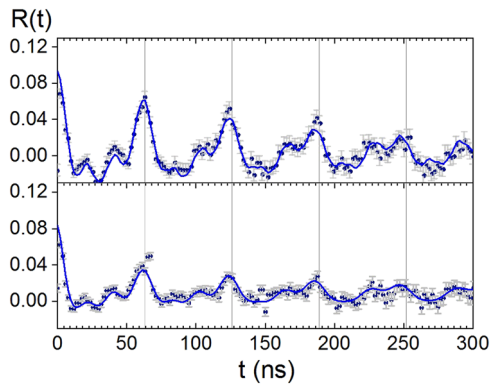

FIG. 3. TDPAC spectra of single-crystal TiO_2 measured at room temperature using ^{111m}Cd(^{111}Cd) as probe nuclei, after RTA at 873 K for 10 minutes in vacuum (bottom) or in O_2 atmosphere (top). The least-squares fits of the hyperfine parameters are represented by the blue solid curves.

The second local environment (B) presents the frequency ω_0 = 294(7) Mrad/s with η = 0.17(1) for δ = 2(4)% and f = 18(5)%. The existence of an oxygen vacancy, in the oxygen octahedron surrounding the impurity, can cause an increase in ω_0, in contrast with the result without vacancy.[39] By comparing our results with those from previous work,[20] on ^{111m}Cd ω_0 = 235(8) Mrad/s with σ = 117(10) Mrad/s or on ^{111m}Cd+^{111}In ω_0 = 257(14) Mrad/s with σ = 68(16) Mrad/s, we were able to associate the observed hyperfine parameters with defects. Therefore, we expect that this local environment is related to non-stoichiometric titanium dioxide and/or Magnéli phases[40] resulting from the thermal treatment in vacuum and implantation processes.

We now discuss the results obtained after RTA in an O_2 atmosphere. The nuclear quadrupole interaction for the main local environment presents a fraction f = 92(8)% for ω_0 = 100(2) Mrad/s with η = 0.20(1) and δ = 4(2)%. The frequency and asymmetry parameters are very close to the local environment (A). In contrast with the other spectrum, the data show a lower damping in modulations of the R(t) function and higher fraction value. This indicates the ease with which Cd occupies regular substitutional Ti-sites upon thermal treatment in O_2.

The second local environment presents a higher frequency, ω_0 = 295(5) Mrad/s, to that of Cd at the substitutional Ti-site associated with a defect, and assumes a lower frequency distribution δ = 1(4)%. In comparison with the local environment (B), its fraction decreased to f = 8(6)%, and the asymmetry parameter η = 0.15(1) assumed similar value. There are two types of effects that should be considered: the non-stoichiometry of the system and the lattice distortions caused by Cd as an impurity. Both interfere in the mechanism of oxygen diffusion.[27]

VII. NEW PERSPECTIVES

This paper briefly describes perturbed angular correlation measurements in titanium dioxide, and we conclude that our investigations address several challenging topics. Results obtained using perturbed angular correlation measurements have generated much interest over the past few decades. Innovative experimental methods, such as those of Banerjee *et al.*[23] who measured TDPAC spectra after exposing titanium dioxide to gamma radiation, highlights important potential applications, such as an immobilizing matrix for nuclear waste. Here we have reported on ^{111m}Cd measurements carried out at ISOLDE-CERN in different annealing atmospheres. The hyperfine parameters were very sensitive to local changes in the non-stoichiometry of rutile, as can be observed in the behavior of the second local environment. Currently, we are investigating local defects in nanostructured TiO_2:H thin films to improve their inherent photocatalytic efficiency.[41]

ACKNOWLEDGMENTS

We acknowledge the financial support received from the Federal Ministry of Education and Research (BMBF) through grants

05K16PGA, 05K16MG3, and 05K16SI1. We also acknowledge the support of all the technical teams at ISOLDE for their excellent work in delivering high-quality beams for TDPAC measurements. We acknowledge the support of the European Union's Horizon 2020 Framework research and innovation program under grant agreement no. 654002 (ENSAR2) given to the ISOLDE experiment IS653. We thank Foundation for Science and Technology FCT, Portugal, via grant CERN-FIS-PAR-0005-2017 and Dr. J. G. M. Correia for technical assistance during the beam time.

REFERENCES

[1] J. Schell, P. Schaaf, and D. C. Lupascu, AIP Adv **7**, 105017 (2017).
[2] P. Schaaf, "Mössbauer Spectroscopy," in *Encyclopedia of Condensed Matter Physics*, edited by G. Bassani, G. Liedl, and P. Wyder (Elsevier–Associated Press, 2005), Vol. 4, pp. 20–31 (ISBN: 0-12-227610-8).
[3] M. Deicher, Hyperfine Interact **79**, 681 (1993).
[4] R. Catherall, W. Andreazza, M. Breitenfeldt, A. Dorsival, G. J. Focker, T. P. Gharsa, T. Giles, J.-L. Grenard, F. Locci, P. Martins, S. Marzari, J. Schipper, A. Shornikov, and T. Stora, J. Phys. G **44**, 094002 (2017).
[5] T. Butz, S. Saibene, Th. Fraenzke, and M. Weber, Nucl. Instrum. Methods Phys. Res. A **284**, 417 (1989).
[6] M. Nagl, U. Vetter, M. Uhrmacher, and H. Hofsäss, Rev. Sci. Instrum. **81**, 073501 (2010).
[7] H. Jaeger, L. Abu-Raddad, and D. J. Wick, Appl. Radiat. Isot. **48**, 1083 (1997).
[8] J. Christiansen, P. Heubes, R. Keitel, W. Klinger, W. Loeffler, W. Sandner, and W. Witthuhn, Z. Phys. B **24**, 177 (1976).
[9] K. Alder and R. M. Steffen, Phys. Rev. **129**, 014434 (1963).
[10] A. Abragam and R. V. Pound, Phys. Rev. **92**, 943 (1953).
[11] H. Frauenfelder, R. M. Steffen, and K. Siegbahn, in α-, β- *and* γ-*Ray Spectroscopy*, edited by K. Siegbahn (North-Holland, 1965).
[12] P. Blaha, K. Schwarz, G. K. H. Madsen, D. Kvasnicka, J. Luitz, R. Laskowski, F. Tran, and L. D. Marks, *WIEN2k, An Augmented Plane Wave + Local Orbitals Program for Calculating Crystal Properties* (Karlheinz Schwarz, Techn. Universität Wien, Austria, 2018), ISBN 3-9501031-1-2.
[13] L. A. Errico, G. Fabricius, M. Renterıa, P. de la Presa, and M. Forker, Phys. Rev. Lett. **89**, 055503 (2002).
[14] L. A. Errico, G. Fabricius, and M. Renterıa, Phys. Rev. B **67**, 144104 (2003).
[15] L. Errico, Hyperfine Interact **158**, 29 (2004).
[16] J. Schell, D. C. Lupascu, A. W. Carbonari, R. D. Mansano, I. S. Ribeiro, Jr., T. T. Dang, I. Anusca, H. Trivedi, K. Johnston, and R. Vianden, J. Appl. Phys. **121**, 145302 (2017).
[17] S.-b. Ryu, S. K. Das, T. Butz, W. Schmitz, C. Spiel, P. Blaha, and K. Schwarz, Phys. Rev. B **77**, 094124 (2008).
[18] T. Butz and R. Vianden, Hyperfine Interact **221**, 99 (2013).
[19] S. K. Das, S. V. Takhare, and T. Butz, J. Phys. Chem. Solids **70**, 778 (2009).
[20] J. Schell, D. C. Lupascu, J. G. M. Correia, A. W. Carbonari, M. Deicher, M. B. Barbosa, R. D. Mansano, K. Johnston, I. S. Ribeiro, Jr., and ISOLDE Collaboration, Hyperfine Interact **238**, 2 (2016).
[21] T. Wenzel, A. Bartos, K. P. Lieb, M. Uhrmacher, and D. Wiarda, Ann. Phys. **504**, 155 (1992).
[22] J. M. Adams and G. L. Catchen, Phys. Rev. B **50**, 1264 (1994).
[23] D. Banerjee, R. Guin, S. K. Das, and S. V. Thakare, J. Radioanal. Nucl. Chem. **290**, 119 (2011).
[24] D. Banerjee, S. K. Das, S. V. Thakare, P. Y. Nabhiraj, R. Menon, R. K. Bhandari, and K. Krishnan, J. Phys. Chem. Solids **71**, 983 (2010).
[25] T. Martucci, J. M. Ramos, A. W. Carbonari, A. S. Silva, and R. N. Saxena, in International Nuclear Atlantic Conference ISBN: 978-85-99141-04-5 (2011).
[26] Y. Mizuno, F. K. King, Y. Yamauchi, T. Homma, A. Tanaka, Y. Takakuwa, and T. Momose, J. Vac. Sci. Technol. A **20**, 1716 (2002).
[27] T. B. Gruenwald and G. Gordon, J. Inorg. Nucl. Chem. **33**, 1151 (1971).
[28] J. W. Rogers, Jr., K. L. Erickson, D. N. Belton, R. W. Springer, T. N. Taylor, and J. G. Beery, Appl. Surf. Sci. **35**, 137 (1988).
[29] G. N. Darriba, L. A. Errico, P. D. Eversheim, G. Fabricius, and M. Rentería, Phys. Rev. B **79**, 115213 (2009).
[30] A. A. Cavalheiro, J. C. Bruno, M. J. Saeki, J. P. S. Valente, and A. O. Florentino, J. Mater. Sci. **43**, 602 (2008).
[31] R. A. Bennett, P. Stone, and M. Bowker, Faraday Discuss **114**, 267 (1999).
[32] A. Zaleska, Recent Patents on Engineering **2**, 157 (2008).
[33] S. H. Othman, S. A. Rashid, T. I. M. Ghazi, and N. Abdullah, J. Nanomater **2011**, 571601.
[34] J. Schell, P. Schaaf, U. Vetter, and D. C. Lupascu, AIP Adv **7**, 095010 (2017).
[35] H. P. Gunnlaugsson, R. Mantovan, H. Masenda, T. E. Mølholt, K. Johnston, K. Bharuth-Ram, H. Gislason, G. Langouche, D. Naidoo, S. Ólafsson, A. Svane, G. Weyer, and the ISOLDE Collaboration, J. Phys. D **47**, 065501 (2014).
[36] S.-M. Chang and R.-A. Doong, J. Phys. Chem. B **110**, 20808 (2006).
[37] D. Banerjee, S. K. Das, P. Das, S. V. Thakare, and T. Butz, Hyperfine Interact **197**, 193 (2011).
[38] Nightmare (MDI) Version RC 3 (1.2.0.247). Copyright (2005-2010) from the Reiner Vianden group, and (2008-2010) Ronan Nédélec, Bonn University.
[39] J. Schell, D. C. Lupascu, A. W. Carbonari, R. D. Mansano, R. S. Freitas, J. N. Goncalves, T. Thanh Dang, and R. Vianden, and the ISOLDE Collaboration," J. Appl. Phys. **121**, 195303 (2017).
[40] L. Liborio and N. Harrison, Phys. Rev. B **77**, 104104 (2008).
[41] D. Zyabkin, J. Schell, D. C. Lupascu, H. Pall Gunnlaugson, H. Masenda, R. Mantovan, K. Baruth Ram, S. Ólafsson, H. P. Gíslason, B. C. Qi, P. Rkastev, J. G. M. Correia, U. Vetter, and P. Schaaf, Hyperfine interactions in hydrogenated TiO_2 thin films and powders for photocatalytic reactions, ISOLDE active experiment IS653, Proposal to the ISOLDE and Neutron Time-of-Flight Committee, ISOLDE-CERN, 2018.